

# Atomic charge distribution in sodosilicate glasses from terahertz time-domain spectroscopy

Edward P. J. Parrott,<sup>1,2,\*</sup> J. Axel Zeitler,<sup>2,†</sup> Guilhem Simon,<sup>3</sup> Bernard Hehlen,<sup>4</sup> Lynn F. Gladden,<sup>2</sup> Sergei N. Taraskin,<sup>5</sup> and Stephen R. Elliott<sup>5</sup>

<sup>1</sup>*Cavendish Laboratory, University of Cambridge, J. J. Thomson Avenue, Cambridge CB3 0HE, United Kingdom*

<sup>2</sup>*Department of Chemical Engineering and Biotechnology, University of Cambridge, Pembroke Street, Cambridge CB2 3RA, United Kingdom*

<sup>3</sup>*Laboratoire de Dynamique, Interactions et Réactivité (LADIR), UPMC Université Paris 06, UMR 7075, 75005 Paris, France*

<sup>4</sup>*Laboratoire des Colloïdes, Verres et Nanomatériaux, Université Montpellier II-CNRS, 34095 Montpellier Cedex 5, France*

<sup>5</sup>*Department of Chemistry, University of Cambridge, Lensfield Road, Cambridge CB2 1EW, United Kingdom*

(Received 23 June 2010; revised manuscript received 5 September 2010; published 26 October 2010)

Terahertz time-domain spectroscopy has been used to extract the light-to-vibration coupling coefficient for sodosilicate glasses, from which it was possible to calculate the variance in the distribution of uncorrelated charges. It was found that increasing the sodium content of the glasses increased the standard deviation of the uncorrelated charge distribution in a linear fashion, and was almost an order of magnitude higher when compared to the charge distribution for pure silica reported previously, in agreement with previously published simulation data.

DOI: [10.1103/PhysRevB.82.140203](https://doi.org/10.1103/PhysRevB.82.140203)

PACS number(s): 63.50.Lm, 61.43.Fs

In recent years, terahertz time-domain spectroscopy (THz-TDS) has emerged as a useful analytical tool in such diverse fields as pharmaceuticals,<sup>1</sup> solid-state chemistry,<sup>2</sup> security monitoring,<sup>3</sup> medical screening,<sup>4</sup> and amorphous materials.<sup>5–9</sup> As a time-domain technique, THz-TDS is able to record both the amplitude and phase of the terahertz electric field, thereby allowing the extraction of the complex refractive index of the sample. In contrast to other techniques that operate in this frequency range, such as Fourier transform infrared spectroscopy, it is not necessary to resort to complex Kramers-Kronig analysis of THz-TDS data for evaluation of the real and imaginary parts of the refractive index. In a previous paper, we have shown that we can obtain estimates for charge-fluctuation values in glasses from THz-TDS.<sup>5</sup> The purpose of this paper is to demonstrate this method for extracting atomic-charge-fluctuation values for sodium silicate glasses with variable sodium concentrations.

Amorphous solids, such as glasses, are materials with a structure lacking in periodicity, extended symmetry, and long-range order. Because of this, the study of these materials presents very different challenges to those for the crystalline materials that have been extensively studied previously using THz-TDS.

Recently, it has been shown that disordered materials (such as amorphous solids) exhibit a universal frequency dependence of the optical absorption in the far-infrared regime.<sup>5</sup> These universal features are due to both the vibrational eigenmodes below the boson peak being similar to plane waves and therefore characterized by a Debye-type vibrational density of states (VDOS),<sup>10,11</sup> and to the presence of fluctuating atomic charges within the sample. The contribution from atomic-charge fluctuations can be split into an uncorrelated, random component due to structural disorder on intermediate and long-range scales, and a correlated component of charge fluctuations caused by variations in the local structure (e.g., Si-O-Si angle in silicate glasses<sup>12</sup>) which obey local charge neutrality within the structural units. The overall frequency dependence of the low-frequency absorp-

tion coefficient,  $\alpha(\omega)$ , is predicted<sup>5</sup> to be of the following form:

$$\alpha(\omega) = C(\omega)g(\omega) \approx \omega^2 C(\omega) = \omega^2(A + B\omega^2), \quad (1)$$

where  $C(\omega)$  is the coupling coefficient for photons and atomic vibrations,  $g(\omega)$  is the VDOS,  $A$  and  $B$  are material-dependent constants describing the uncorrelated and correlated charges, respectively. Concentrating on the uncorrelated charges, it can be shown that the variance of the uncorrelated charge distribution ( $\sigma_1^2$ ) is related to the  $A$  coefficient through the following expression:<sup>8</sup>

$$\sigma_1^2 = \frac{A\bar{m}c_0\sqrt{\epsilon_\infty}}{2\pi^2n}, \quad (2)$$

where  $\bar{m}$ ,  $\epsilon_\infty$ , and  $n$  are the average atomic mass, the high-frequency limit of the ionic dielectric constant, and the atomic concentration, respectively, and  $c_0$  is the speed of light in a vacuum. A measure of the variance of the charge distribution gives a useful insight into the relative ionicities of the atoms, with larger variances suggesting greater differences in atomic charges between atoms.

In this Rapid Communication, a series of sodosilicate glasses, with chemical formula  $\xi\text{Na}_2\text{O} \cdot (1-\xi)\text{SiO}_2$  and  $\xi$  being set at 0.33, 0.25, and 0.2 (hereafter referred to as NS2, NS3, and NS4, respectively) are investigated using THz-TDS in order to measure the low-frequency dielectric behavior, in particular, the absorption coefficient ( $\alpha$ ). Using the same techniques as reported previously<sup>9</sup> the optical constants of the NS2, NS3, and NS4 glasses were extracted from the THz-TDS data. From the frequency dependence of the absorption coefficient in the far-infrared range, the coupling coefficient between far-infrared photons and atomic vibrations in different sodosilicate glasses has been calculated as a function of frequency, and its low-frequency limit, i.e., the value of the parameter  $A$ , has been obtained. Finally, the value of  $A$  has been used to estimate the typical width of the uncorrelated charge distribution,  $\sigma_1$ , by employing Eq. (2).

TABLE I. The composition ratio, mole fraction of sodium, sample thickness, densities, and average molecular mass for the three sodosilicate glasses,  $\xi\text{Na}_2\text{O} \cdot (1-\xi)\text{SiO}_2$  measured herein.

Identifier	$\xi$	$x_{\text{Na}}^a$	$d^b$ (mm <sup>-1</sup> )	$\rho^c$ (g cm <sup>-3</sup> ) <sup>-1</sup>	$\bar{m}^d$ (g)
NS2	0.33	0.22	0.180, 0.835	2.49	$3.361 \times 10^{-23}$
NS3	0.25	0.17	0.320, 0.972	2.43	$3.352 \times 10^{-23}$
NS4	0.20	0.13	0.150	2.38	$3.347 \times 10^{-23}$

<sup>a</sup>Sodium mole fraction.

<sup>b</sup>Sample thickness.

<sup>c</sup>Glass densities taken from the work of Doweidar (Ref. 14).

<sup>d</sup>Average molecular mass.

The glasses investigated were synthesized from fine quartz and sodium carbonate powders melted in platinum crucibles in an electric muffle furnace as described previously.<sup>13</sup>

The terahertz time-domain waveforms were acquired using a setup described previously.<sup>2</sup> Briefly, subpicosecond coherent pulses of broadband terahertz radiation (0.1–4 THz) were generated by photoexcitation of a dc-biased semi-insulating GaAs substrate by 12 fs pulses of a near-infrared laser (Femtolasers, Femtosource cM1, Vienna, Austria, center wavelength 800 nm). The pulsed terahertz radiation was transmitted through the glass sample and detected using electro-optic sampling with a ZnTe crystal.

The optical constants were extracted from the THz-TDS time-domain data using an algorithm similar to the multiple-reflection extraction method reported previously for As<sub>2</sub>S<sub>3</sub>.<sup>9</sup> However, in contrast to that work, the optical constants were extracted here by comparing the difference between the terahertz electric field recorded for a reference measurement in air with that obtained after propagation through the glass material. Where possible, two different thicknesses were used for each of the glass samples: the thinner sample allowed higher frequency data to be obtained, whereas the thicker sample improved the accuracy of the low-frequency data due to the larger interaction length. The sample thicknesses measured are detailed in Table I. For the NS4 case, the thicker sample was not suitable for measurement using THz-TDS and so for this case only the results obtained for a single thin sample are reported. For the NS2 and NS3 results reported herein, the optical constants are a combination of those extracted for the thicker sample at low frequencies ( $\leq 0.9$  THz, thick sample) with those extracted at higher frequencies ( $> 0.9$  THz, thin sample).

Figures 1(a) and 1(b) report the absorption coefficients and real parts of the refractive indices extracted from the THz-TDS data of the NS2, NS3, and NS4 glasses. Focusing initially on the refractive index results in Fig. 1(b), clear differences are observed in the value of the refractive index obtained for the three samples, with the refractive index values at 1 THz being 2.78, 2.59, and 2.34 for the NS2, NS3, and NS4 glasses, respectively. Consideration of the relative concentrations of Na<sub>2</sub>O to SiO<sub>2</sub> in these materials reveals that the increase in refractive index follows the increase in Na<sub>2</sub>O concentration within the glasses. This trend of increasing refractive index with Na<sub>2</sub>O concentration is consistent with refractive index data published for pure SiO<sub>2</sub> with only

trace inclusions of elements other than silicon and oxygen, where a refractive index of  $\approx 1.95$  at 1 THz has been reported by Naftaly and Miles.<sup>7</sup>

The absorption coefficient data [Fig. 1(a)] also reveal substantial differences between the three glasses at terahertz frequencies. All three glasses display terahertz absorption coefficients which increase across the frequency range, as expected for amorphous materials. Below  $\approx 1$  THz, differences are difficult to resolve upon a cursory examination; however closer study reveals a slightly larger gradient for NS2 compared to NS3 and a larger difference is apparent in the gradient of the NS4 data. These different gradients result in a larger observable difference between the three materials at higher frequencies (above  $\approx 1.2$  THz). In the absorption coefficient data recorded for NS4, there also appears to be a broad feature (change in slope) centered around  $\approx 1$  THz. This feature, perhaps, can be associated with the boson peak where the nature of vibrational eigenmodes changes from being weakly hybridized (below the boson peak) to strongly hybridized plane waves with a possible mixture of local components (above the boson peak).<sup>15</sup> Similar features might be expected in the frequency dependence of the absorption

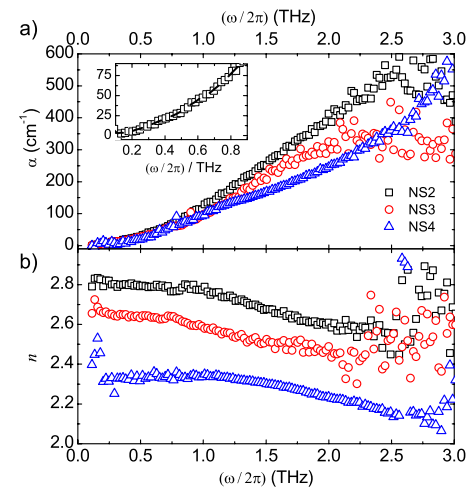


FIG. 1. (Color online) (a) Absorption coefficient data for the three NS glass samples between 0.1 and 3 THz. The inset shows the NS2 glass data at low frequencies where the black dashed line represents the smoothed absorption data used for the later analysis of the coupling coefficient. (b) Refractive index data for the three NS glasses between 0.1 and 3 THz.

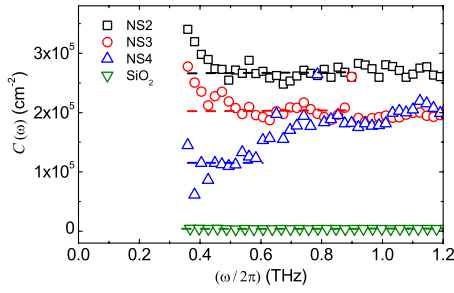


FIG. 2. (Color online) A plot of the coupling coefficient  $C(\omega)$  extracted for the three glasses as a function of frequency between 0.1 and 1.2 THz, along with the coupling coefficient data for  $\text{SiO}_2$  published previously (Ref. 5). The dashed lines represent the fits to Eq. (1) calculated from these data using  $\beta_0=3.4$ . Only the data below the boson peak were included in the fit ( $\text{NS2} \leq 0.9$  THz,  $\text{NS4} \leq 0.6$  THz).

coefficients for NS2 and NS3 glasses but they are not seen so clearly, possibly due to a different location and a weaker strength of the boson peak in these materials. This observation agrees with the measurement of the boson peak of NS2 and NS4 glasses using Raman spectroscopy reported previously, where a decrease in the strength, and increase in the frequency, of the boson peak was observed when comparing the NS2 glass to the NS4 glass.<sup>16</sup> For comparison, the absorption coefficient for pure glassy  $\text{SiO}_2$  has been reported by numerous studies<sup>5-7</sup> to be below  $5 \text{ cm}^{-1}$  across the entire frequency range probed in the present experiment. These published results agree with the observed trend toward increasing absorption coefficient with increasing concentration of  $\text{Na}_2\text{O}$  observed in the data presented here.

The absorption coefficient data were smoothed using a moving-average filter (each point being the average of five nearest neighbors) in order to facilitate the extraction of the coupling coefficients for the glasses. The results for this operation are highlighted in the inset in Fig. 1 where it can be seen that the smoothed absorption data for the NS2 glass preserve the low-frequency behavior of the absorption coefficient.

In order to calculate the coupling coefficient from the THz-TDS absorption data displayed in Fig. 1(a), an independent measure of the VDOS is required. For the NS2 and NS3 glasses, the VDOS used were those which have recently been calculated from the low-temperature heat-capacity behavior,<sup>17</sup> whereas the previously reported VDOS calculated using a Car-Parrinello *ab initio* model was used for the NS4 glass.<sup>18</sup> The reduced VDOS,  $g(\omega)/g_D(\omega) = \beta(\omega)$  [where  $g_D(\omega)$  is the Debye VDOS with Debye frequencies reported in Ref. 19], in sodosilicate glasses exhibits the boson peak around 1 THz and approaches its limiting value  $\beta(\omega \rightarrow 0) = \beta_0 > 1$  in the low-frequency regime. The value of  $\beta_0$  is not yet available experimentally for these glasses (moreover, the VDOS in Ref. 17 is not normalized to the simulation size). Therefore, the range of values and the VDOS in Ref. 18 could suffer significantly at low frequencies from finite-size effects due  $\beta_0^{\min} \leq \beta_0 \leq \beta_0^{\max}$ , with  $\beta_0^{\min} = 2$  (see Ref. 20) and  $\beta_0^{\max} = 3.4$  (see Ref. 5) have been used in our analysis (see Fig. 3).

Figure 2 displays the coupling coefficients extracted for

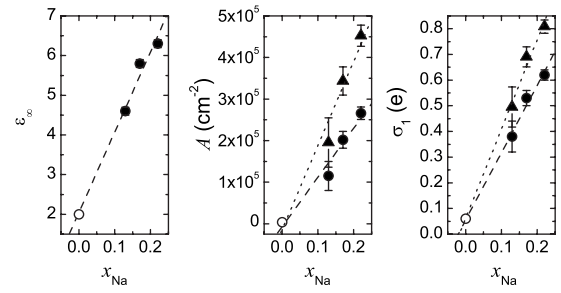


FIG. 3. The values of  $\epsilon_\infty$ ,  $A$  and the standard deviation of the uncorrelated charge distribution,  $\sigma_1$ , as a function of Na concentration. The error bars represent the uncertainty in  $\sigma_1$  as a result of the experimental uncertainty in the value of  $A$  and  $\epsilon_\infty$ . Filled circles (triangles in middle and right panels) are the values calculated in this paper for  $\beta_0=3.4$  ( $\beta_0=2$ ), and the open circle is the value calculated for  $\text{SiO}_2$  previously (Ref. 5). The straight lines through the points represent best linear fits to the data.

the three NS glasses as a function of frequency. In order to calculate the coupling coefficient, only the data below the approximate positions of the boson peak were used to fit Eq. (1), as this relationship is not necessarily expected to hold true for frequencies above the boson peak. For the coupling coefficient obtained for the NS2 and NS3 glasses, data points below  $\approx 0.9$  THz were used; however, for the coupling-coefficient data of the NS4 glass, the boson peak is apparent around this frequency and so only the data points below  $\approx 0.6$  THz were used. Values for  $A$ , the coefficient attributed to uncorrelated charges, of  $(2.66 \pm 0.15) \times 10^5 \text{ cm}^{-2} < A < (4.52 \pm 0.26) \times 10^5 \text{ cm}^{-2}$ ,  $(2.02 \pm 0.20) \times 10^5 \text{ cm}^{-2} < A < (3.43 \pm 0.34) \times 10^5 \text{ cm}^{-2}$ , and  $(1.15 \pm 0.35) \times 10^5 \text{ cm}^{-2} < A < (1.96 \pm 0.60) \times 10^5 \text{ cm}^{-2}$  were extracted from the data for the NS2, NS3, and NS4 glasses, respectively (values for  $A$  and its experimental error assuming  $\beta_0=3.4$  or  $\beta_0=2$ , respectively). The value of the  $B$  coefficient was not determined accurately due to the small frequency range measured but appeared to be approaching zero in all three cases, which agrees with the small value,  $B \approx 0.3 \text{ cm}^{-1}$ , extracted for glassy  $\text{SiO}_2$  previously.<sup>5</sup> That the  $B$  coefficient does not change significantly with sodium concentration suggests that the correlated charge fluctuations are not affected by the sodium inclusions.

A measure of the charge distribution as afforded by  $\sigma_1$  may be found using the expression in Eq. (2). The values of  $\bar{m}$ ,  $c_0$ , and  $n = \rho/\bar{m}$  (where  $\rho$  is the glass density) are all known or may be calculated from other known constants (see Table I). The value of  $\epsilon_\infty$  was taken to be the value of the high-frequency limit of the dielectric constant as measured using THz-TDS, and was found to lie between 4.6 and 6.3 for the three glasses. Using the value of  $A$  calculated previously, values for  $\sigma_1$  were found to be  $(0.62 \pm 0.02)e < \sigma_1 < (0.81 \pm 0.03)e$ ,  $(0.53 \pm 0.03)e < \sigma_1 < (0.69 \pm 0.04)e$ , and  $(0.38 \pm 0.06)e < \sigma_1 < (0.50 \pm 0.08)e$  for NS2, NS3, and NS4, respectively (values for  $\sigma_1$  and its experimental error assuming  $\beta_0=3.4$  or  $\beta_0=2$ , respectively). These values, along with  $\sigma_1$  calculated for  $\text{SiO}_2$  previously,<sup>5</sup> are plotted in Fig. 3 as a function of the molar fraction of sodium. As can be seen in Fig. 3, the value of  $\sigma_1$  appears to be influenced to a large extent by the addition of  $\text{Na}_2\text{O}$  into the  $\text{SiO}_2$  framework,

with an order-of-magnitude increase in the value of  $\sigma_1$  when compared to that of pure  $\text{SiO}_2$  (0.06e).

In addition, there appears to be an approximately linear relationship between the mole fraction of sodium and the value of  $\sigma_1$ . A possible interpretation of this effect is as follows. It is known that the addition of sodium ions in silica results in the formation of nonbridging oxygen, i.e.,  $\text{Si-O}\cdots\text{Na}$  configurations, contrasted with bridging oxygen configurations,  $\text{Si-O-Si}$ . Consequently, the addition of sodium species leads to a nonlocal redistribution of all the atomic charges, resulting in a weakening of Si-O bonds.<sup>21–23</sup> The fact that  $B$  is insensitive to the increasing concentration of sodium atoms implies that the effect of the sodium atoms on the charge redistribution appears to be nonlocalized. This suggests that the role of the correlated charge fluctuations responsible for the quadratic frequency term in Eq. (1) is suppressed in sodium silicates. In contrast, the long-range uncorrelated charge fluctuations, and thus the value of  $\sigma_1$ , are expected to be enhanced with increasing concentration of Na ions. Further analysis of the role of the sodium inclusions on the distribution of charge requires higher quality VDOS data at low frequencies, in order to constrain further the value of  $\beta_0$ .

In this Rapid Communication, we have presented a systematic study into the atomic charge distribution of a series

of sodosilicate glasses using THz-TDS. As a time-domain technique, it is possible to extract both the refractive index and absorption coefficient directly. By using the universal frequency dependence of the absorption introduced previously,<sup>5</sup> and an independent estimation of the VDOS, the coupling coefficients relating to both correlated and uncorrelated charges can be extracted. In particular, we have used the uncorrelated coefficient ( $A$ ) to extract a measure of the distribution of uncorrelated charges within the NS glasses ( $\sigma_1$ ). An order of magnitude increase in  $\sigma_1$  was observed in the NS glasses when compared to pure  $\text{SiO}_2$ . There appears to be a linear relationship between  $\sigma_1$  and the mole fraction of sodium, possibly suggesting that the uncorrelated charge fluctuations are dominated by the spatial disorder of the positions of the sodium atoms.

The authors would like to acknowledge C. Dupas for sample preparation and P. Richet for the synthesis of the sodosilicate glasses. E.P.J.P., J.A.Z., and L.F.G. would like to thank the RCUK Basic Technology Programme (Grant No. EP/E048811/1) for funding. Furthermore J.A.Z. would like to acknowledge Gonville & Caius College, Cambridge. G.S. and B.H. would like to thank PHC Alliance 14998VC for support.

\*Present address: Department of Electronic Engineering, Chinese University of Hong Kong, Shatin N.T., Hong Kong.

†jaz22@cam.ac.uk

- <sup>1</sup>J. A. Zeitler, P. F. Taday, D. A. Newnham, M. Pepper, K. C. Gordon, and T. Rades, *J. Pharm. Pharmacol.* **59**, 209 (2007).
- <sup>2</sup>E. P. J. Parrott, J. A. Zeitler, T. Friscic, M. Pepper, W. Jones, G. M. Day, and L. F. Gladden, *Cryst. Growth Des.* **9**, 1452 (2009).
- <sup>3</sup>J. F. Federici, B. Schulkin, F. Huang, D. Gary, R. Barat, F. Oliveira, and D. Zimdars, *Semicond. Sci. Technol.* **20**, S266 (2005).
- <sup>4</sup>E. Pickwell and V. P. Wallace, *J. Phys. D: Appl. Phys.* **39**, R301 (2006).
- <sup>5</sup>S. N. Taraskin, S. I. Simdyankin, S. R. Elliott, J. R. Neilson, and T. Lo, *Phys. Rev. Lett.* **97**, 055504 (2006).
- <sup>6</sup>D. Grischkowsky, S. Keiding, M. van Exter, and C. Fattinger, *J. Opt. Soc. Am. B* **7**, 2006 (1990).
- <sup>7</sup>M. Naftaly and R. Miles, *J. Non-Cryst. Solids* **351**, 3341 (2005).
- <sup>8</sup>S. N. Taraskin, *J. Phys.: Condens. Matter* **19**, 415113 (2007).
- <sup>9</sup>E. P. J. Parrott, J. A. Zeitler, L. F. Gladden, S. N. Taraskin, and S. R. Elliott, *J. Non-Cryst. Solids* **355**, 1824 (2009).
- <sup>10</sup>S. N. Taraskin and S. R. Elliott, *Phys. Rev. B* **61**, 12017 (2000).
- <sup>11</sup>S. N. Taraskin and S. R. Elliott, *Phys. Rev. B* **61**, 12031 (2000).

- <sup>12</sup>D. Donadio, M. Bernasconi, and F. Tassone, *Phys. Rev. B* **70**, 214205 (2004).
- <sup>13</sup>P. Richet, Y. Bottinga, and C. Téqui, *J. Am. Ceram. Soc.* **67**, C6 (1984).
- <sup>14</sup>H. Doweidar, *J. Non-Cryst. Solids* **194**, 155 (1996).
- <sup>15</sup>S. N. Taraskin, Y. L. Loh, G. Natarajan, and S. R. Elliott, *Phys. Rev. Lett.* **86**, 1255 (2001).
- <sup>16</sup>C. Chemarin and B. Champagnon, *J. Non-Cryst. Solids* **243**, 281 (1999).
- <sup>17</sup>N. F. Richet, *Physica B* **404**, 3799 (2009).
- <sup>18</sup>S. Ispas, N. Zotov, S. Dewispelaere, and W. Kob, *J. Non-Cryst. Solids* **351**, 1144 (2005).
- <sup>19</sup>N. Zotov, *J. Phys.: Condens. Matter* **14**, 11655 (2002).
- <sup>20</sup>G. Baldi, A. Fontana, G. Monaco, L. Ohrsingher, S. Rols, F. Rossi, and B. Ruta, *Phys. Rev. Lett.* **102**, 195502 (2009).
- <sup>21</sup>S. Ispas, M. Benoit, P. Jund, and R. Jullien, *Phys. Rev. B* **64**, 214206 (2001).
- <sup>22</sup>T. Uchino, M. Iwasaki, S. Sakka, and Y. Ogata, *J. Phys. Chem.* **95**, 5455 (1991).
- <sup>23</sup>T. Uchino, S. Sakka, Y. Ogata, and M. Iwasaki, *J. Phys. Chem.* **97**, 9642 (1993).